

6. A. Ya. Belen'kii and A. F. Shevalin, "Calculation of electric field gradients around the nuclei in elastically deformed metals," *Fiz. Met. Metalloved.*, 45, No. 3 (1978).
7. G. N. Belozerskii and V. G. Semenov, "Mössbauer investigations of the spin texture of the surface of amorphous ferromagnets," *Fiz. Tverd. Tela (Leningrad)*, 27, No. 6 (1985).

SPECTRAL COMPOSITION OF LIGHT SCATTERED IN FLUID FLOW AROUND
A ROTATING DISK

V. A. Bazanov, N. A. Rubtsov, and V. P. Solov'ev

UDC 535.3:532.517

The experimental investigation of the spectral composition of laser radiation scattered by a volume of turbulent fluid motion is a widespread means of studying the spatial and temporal correlations of thermodynamic parameters and turbulent velocity fluctuations characterizing fluid flow. The results provide information about the amplitude, characteristic frequencies, and lifetimes of these fluctuations. Such experiments can be used to obtain data on very small fluctuation scales (which are not accessible to investigation by other methods) of turbulent origin without introducing disturbances in the investigated flow. They can be divided into two groups according to the nature of the scattering inhomogeneities: 1) scattering by particles that are introduced artificially or exist naturally in the flow, where the intensity of the particle-scattered light is much greater than the intensity of light scattered by fluctuations of the dielectric constant of the medium; 2) scattering in a pure fluid by turbulent fluctuations of the refractive index in the flow itself.

The first group exploits the well-developed methods of laser Doppler anemometry, which are widely used in present-day experimental fluid dynamics [1, 2].

Development of the second group has been thwarted by the difficulties of creating flow of a pure fluid and the low intensity of the radiation scattered by density fluctuations. However, strong light scattering is possible in well-developed turbulent fluid flow, even without suspended particles. The feasibility of such an investigation was first noted by Frisch [3], who estimated that the ratio of the turbulence-induced scattered light intensity to the molecular scattering intensity becomes greater than unity for sufficiently large Reynolds numbers.

It has been brought to our attention [4, 5] that experiments of this kind could prove to be most interesting. The wave number q of the scattering vector corresponds to the characteristic space scale of scattering inhomogeneities $\ell = 1/q$. The scattering angle θ is related to the wave number q by the Bragg equation $q = (2/\lambda)\sin(\theta/2) = 2k\sin(\theta/2)$ (λ is the wavelength of the incident radiation). Accordingly, by varying the scattering angle it is possible to investigate the regions corresponding to a large set of scales of cascade-decaying vortices, all the way from the outer turbulence scale L down to the smallest vortex length ℓ_m and the dissipation interval $q > 1/\ell_m$. Larger-scale fluctuations are observed by decreasing the angle, and smaller-scale fluctuations are observed by increasing it. The width of the scattering line should yield information about the lifetime of the scattering fluctuations in this case. Consequently, by studying dynamic light scattering in a pure fluid, we obtain information not only about the velocity distribution in turbulent flow, but also about the nature of the damping of turbulent fluctuations.

1. Laser Heterodyne Spectroscopy. The spectral composition of the scattered radiation can be investigated experimentally by laser heterodyne (optical mixing) spectroscopy, in which part of the unscattered laser beam is used as a reference beam for mixing with the scattered radiation on the surface of a photodetector. The output in this case is an electric signal proportional to the modulus squared on the total electric field incident on the sensing area of the photodetector. We write the electric field vector of the radiation in

the form $\mathbf{E}(\mathbf{r}, t) = \mathbf{E}_0(\mathbf{r}, t) + \mathbf{E}_S(\mathbf{r}, t)$ [$\mathbf{E}_0(\mathbf{r}, t) = \mathbf{E}_0 \exp(i\omega_0 t)$ is the incident reference field, and \mathbf{E}_S is the scattered field]. Assuming that the fields of the scattered and incident radiation are statistically independent and spatially coherent within the limits of the sensing area of the photodetector and that the intensity of the reference beam is much greater than the intensity of the scattered beam, we determine the correlation function of the photocurrent from the equation [1, 5]

$$R_j(\tau) = \langle j(t)j(t+\tau) \rangle = \left(G \frac{e\eta}{h\nu}\right)^2 R_{j_0}(\tau) + j_0 j_S + R_n(\tau) + \\ + j_0 \left(G \frac{e\eta}{h\nu}\right) \sigma^2 \langle \mathbf{E}_S(\mathbf{r}_1, t) \mathbf{E}_S^*(\mathbf{r}_2, t+\tau) \rangle_{\mathbf{V}} \exp(-i\mathbf{q}\mathbf{V}t) + \\ + j_0 \left(G \frac{e\eta}{h\nu}\right) \sigma^2 \langle \mathbf{E}_S^*(\mathbf{r}_2, t) \mathbf{E}_S(\mathbf{r}_1, t+\tau) \rangle_{\mathbf{V}} \exp(i\mathbf{q}\mathbf{V}t), \quad (1.1)$$

where G is the gain of the photodetector, e is the electron charge, η is the photoelectron quantum efficiency, $h\nu$ is the optical quantum energy, σ is the irradiated surface area of the photodetector, $R_n(\tau)$ is the noise correlation function, j_0 and j_S are the average photocurrent components induced by the separate action of the fields \mathbf{E}_0 and \mathbf{E}_S , and the subscript \mathbf{V} indicates that the quantity in the angle brackets is evaluated in a coordinate system moving with the velocity \mathbf{V} .

The power spectrum of the photocurrent $S(q, \omega)$ is related to the correlation function $R_j(\tau)$ by the Wiener-Khintchine theorem [4]:

$$S(q, \omega) = \frac{1}{2\pi} \int_{-\infty}^{\infty} \exp(iq\tau) R_j(\tau) d\tau.$$

It is evident from Eq. (1.1) that, apart from the zero-frequency component associated with the mutual influence of the reference and scattered beams, $S(q, \omega)$ also has two symmetrical components at the Doppler frequencies $\pm f_D = \mathbf{q} \cdot \mathbf{V}$:

$$S(q, \omega) = j_0 \left(G \frac{e\eta}{h\nu}\right) \frac{\sigma^2}{2\pi} \int_{-\infty}^{\infty} \langle \mathbf{E}_S(\mathbf{r}_1, t) \mathbf{E}_S^*(\mathbf{r}_2, t+\tau) \rangle_{\mathbf{V}} \exp(-i(\omega - f_D)\tau) d\tau + \\ + j_0 \left(G \frac{e\eta}{h\nu}\right) \frac{\sigma^2}{2\pi\nu} \int_{-\infty}^{\infty} \langle \mathbf{E}_S^*(\mathbf{r}_2, t) \mathbf{E}_S(\mathbf{r}_1, t+\tau) \rangle_{\mathbf{V}} \exp(-i(\omega + f_D)\tau) d\tau,$$

which characterize the scattered field and are the components of interest to us.

We shall assume below that scattering is induced in the moving fluid by homogeneous isotropic turbulent fluctuations of the refractive index. It has been shown [6] that scattering in the case of thermostatted flow around a rotating disk is determined by pressure fluctuations, and its intensity is expressed in terms of the scalar spectral density of the velocity fluctuations: $E(q, \tau) = 4\pi q^2 \sigma(q) \exp[-\omega(q)\tau]$ [7]. Here the spectrum of the recorded Doppler signal has the form $S(q, \omega) = A(q)/[(\omega - f_D)^2 + \omega^2(q)]$, where $A(q)$ depends on the scattering geometry and the thermodynamic properties of the medium, and $\omega(q)$ corresponds to the reciprocal of the transfer time of kinetic energy from vortices of scale q^{-1} to vortices of scale $(2q)^{-1}$ in the inertial interval of wave numbers and is given by the equation [7] $\omega(q) = 0.42\varepsilon^{1/3}q^{2/3}$, while in the dissipation interval $q > 1/\ell_m$ it is given by the equation $\omega(q) = \nu q^2$ (ε is the average rate of dissipation of kinetic energy, and ν is the kinematic viscosity).

Thus, the component of the power spectrum of the photodetector output signal at the Doppler frequency $f_D = \mathbf{q} \cdot \mathbf{V} = 2kv \sin(\theta/2)$ has a Lorentzian shape with a half-width exactly equal to $\omega(q)$.

2. Apparatus for Investigating the Spectral Composition of Radiation Scattered in Fluid Flow around a Rotating Disk. The experimental arrangement is shown schematically in Fig. 1 and consists of three main units: a mechanical section, which generates fluid flow around a rotating disk; an optical section, which records the scattered radiation; instrumentation for determining the spectral properties of the scattered radiation.

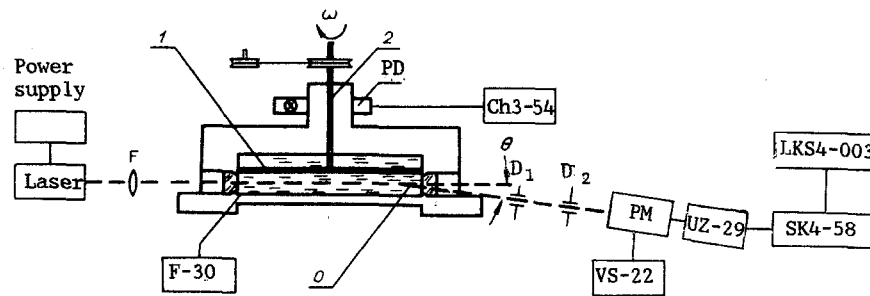


Fig. 1

The main components of the mechanical section are made of Duralumin and are darkened in Fig. 1. The disk 1 of radius 5 cm with the bearing-centered shaft 2 is rotated by a belt drive connected to a dc motor. The casing of the apparatus has viewing windows, an orifice for the insertion of thermocouples, and devices to permit the insertion of a fine wire for alignment purposes. A hole is drilled through the shaft of the disk so that the rotation speed can be measured from the tracking frequency of electrical pulses from a small light source to an FD-10G photodiode (PD), which are recorded by a Ch3-54 frequency meter. The apparatus is mounted on a large optical bench.

The optical section of the apparatus is designed to measure the directional dependence and spectral composition of the scattered radiation. The laser beam (LG-79 or LG-38) is focused by the lens F ($f = 300$ mm) at the point O. Circular diaphragms D_1 and D_2 (with diameters 0.1 mm and 0.15 mm) are used to form the scattering volume. The cylindrical casing of the diaphragms is mounted in positioning racks to align the plane of the diaphragms perpendicular to the direction of the incident radiation. The racks are attached to micrometer stages, which can be moved in three directions and are mounted on the optical bench. The uncertainty $\delta\theta$ of the angle of collection of the scattered radiation did not exceed $5 \cdot 10^{-4}$. The diaphragms were aimed precisely at the center of the scattering volume by means of a fine wire, which was inserted by a special holder from the casing of the apparatus and onto which the beams were directed from the reference laser and from an auxiliary LGN-105 laser set up in place of the photomultiplier (PM), and also by means of mutual alignment of the diaphragms relative to the incident radiation with the aid of the micrometer stages.

Inasmuch as the scattered radiation was investigated at small angles ($0.8^\circ \leq \theta \leq 1.4^\circ$), the radiation scattered elastically by the windows in the cell served adequately as the reference beam in the laser heterodyne method and for achieving amplification of the scattered signal when the photocurrent from the photomultiplier was recorded.

The influence of chemical and mechanical impurities on the scattering of light was minimized by careful two-stage purification of the working liquid (ethyl alcohol) poured into the apparatus: first by vacuum distillation and then by purification through nuclear filters (with a maximum pore diameter of $0.03 \mu\text{m}$).

The scattered radiation receiver was an FEU-79 photomultiplier, whose output signal was sent through a wideband amplifier to an SK4-58 spectrum analyzer. The spectrum was recorded on an LKS4-003 recorder and by photographing the screen of the spectrum analyzer.

The error of measurement of the broadening of the Doppler component of the scattered signal spectrum was associated with additional spectral broadening as a result of many factors: the finiteness of the solid angle in which the analyzed radiation was received; the finite transit time of inhomogeneities through the scattering volume, the velocity gradient within the boundaries of the measured volume, and the finite bandwidth of the narrowband filter of the spectrum analyzer.

It is practically impossible to give a precise estimate of the error of the measured signal. According to recent data [8], the experimentally measured and theoretically estimated measurement errors attributable to the above-indicated factors for turbulent fluid flow agree within $\pm 16\%$ error limits. An analysis [9] indicates that the finiteness of the solid angle of collection of the investigated radiation is the principal cause of broadening of the measured signal. The frequency broadening induced by the fact that light incident on the photodetector corresponds to scattering within the limits of the collection angle φ , rather than at just one angle θ is estimated from the equation $\Delta f_D = (\varphi/\theta)f_D$ (for our appa-

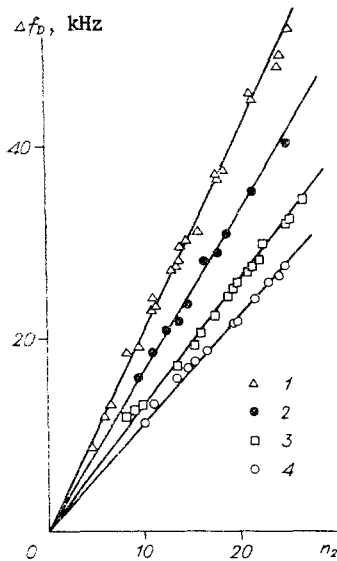


Fig. 2

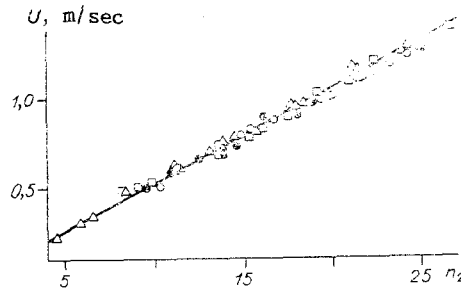


Fig. 3

ratus at $\theta(1^\circ) = 1.7 \cdot 10^{-2}$, $\varphi = 4.7 \cdot 10^{-4}$, $\varphi/\theta = 2.7 \cdot 10^{-2}$, and at typical measured frequencies $f = 10-50$ kHz the resolution of the optical circuit was $\Delta f = 0.27-1.4$ kHz).

3. Measurement of the Average Fluid Flow Velocity. In accordance with the experimental conditions, the center of the scattering volume was located at the same distance $h = 0.005$ m from the rotating disk and from the stationary bottom and at a distance $R_1 = 0.034$ m from the axis of rotation. Figure 2 shows the results of measurements of the Doppler frequency shift of the scattered radiation as a function of the angular velocity of the disk $\omega = \pi n_2$ (n_2 is twice the disk rotation frequency) and the scattering angle (points 1-4 for $\theta = 1.4^\circ, 1.15^\circ, 0.9^\circ$, and 0.8°). It was established that the frequency shift f_D depends linearly on the disk rotation speed with a slight tendency to decrease at the maximum speeds. According to the Bragg condition, these linear dependences shift toward higher frequencies as the scattering angle increases.

The rotation speed and the distance between the disk and the base were large enough for the scattering volume to be located in the main flow region between the boundary layers adjacent to the surfaces of the disk [the thickness of this region is $\delta \sim (\nu/\omega)^{1/2}$]. We know [10] that this intermediate layer rotates like a rigid body with a velocity roughly equal to half the disk rotation speed. Figure 3 shows the tangential component of the fluid velocity U as a function of the disk rotation speed n_2 , as determined from the Doppler shift of the scattered radiation for various scattering angles (the angles correspond to Fig. 2) according to the equation $U = f_D/2k \sin(\theta/2)$. The ratio of the angular velocities of the disk and the core of the main flow was found to be $\omega'/\omega = 0.488$ in this case.

4. Broadening of the Doppler Component of the Scattered Radiation Spectrum. Pictures of the Doppler component of the scattered radiation spectrum, taken from the screen of the SK4-58 spectrum analyzer, can be used to obtain a quantitative estimate of the spectral broadening, which corresponds exactly to the reciprocal lifetime of the scattering density fluctuations, $\Delta f_D = \omega(q) = 1/\tau(q)$.

Figure 4 gives the results of measurements of the half-width of the Doppler component as a function of the fluid flow velocity for various scattering angles. At small flow velocities the broadening is approximately constant, but begins to increase as the flow velocity increases. If we use the estimate for $\omega(q)$ in the case of turbulent flow, we see that the measured values approach this dependence (dashed lines) with increasing scattering angle for $q < q_d$, obviously because a large angle corresponds to a large scattering wave number and, hence, to small inhomogeneities, which correspond in large measure to the model of small-scale turbulence. At small velocities, such that the inhomogeneities do not have sufficient kinetic energy to induce a cascade vortex breakup process, the broadening is approximately consistent with the law of inverse proportionality to the time for kinetic energy to be dissipated into heat, $\omega(q) = \nu q^2$.

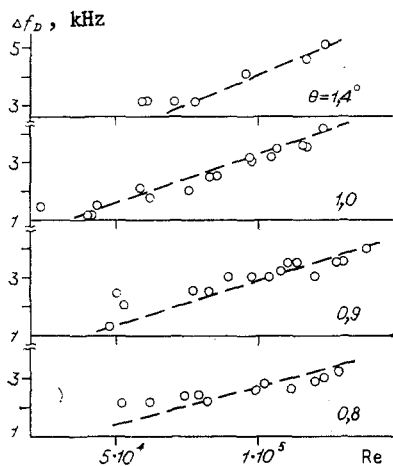


Fig. 4

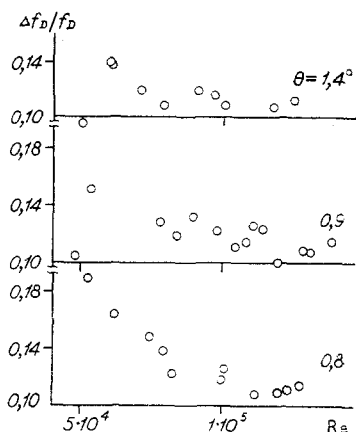


Fig. 5

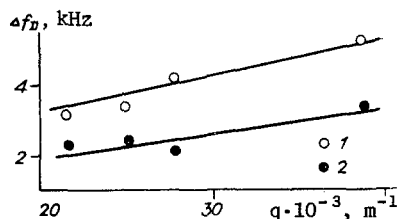


Fig. 6

The dependences for $\omega(q)$ were obtained on the assumption of well-developed turbulent flow, but it follows from [11, 12] that the fluid flow velocities attained for the given dimensions of the apparatus and disk rotation speeds are insufficient for the transition to turbulent flow. The experimental results in [11, 12] corresponding to the theoretical estimates were obtained on precision apparatus with carefully polished and centered disks and give values of the Reynolds numbers at the transition point $Re = (2.6-3.2) \cdot 10^5$. Our apparatus is not so ideal (it contains a number of perturbing elements, such as windows and thermocouples, which accelerate mixing), and the transition to turbulent flow sets in somewhat earlier for it. The relative broadening $\Delta f_D/f_D$ of the Doppler component is sensitive to the time of transition to turbulent flow, increasing abruptly at the critical time. It is evident from Fig. 5, which shows the relative broadening of the spectrum as a function of the flow velocity and $Re = \omega R^2/\nu$ for various scattering angles, that such an increase occurs in the vicinity of $R = 5.2 \cdot 10^4$, which can also correspond to the critical Reynolds number for loss of stability of the turbulent flow regime $((3-9) \cdot 10^4$ [11]), and it could be the start of turbulent flow generation in our situation.

An increase in the scattering angle corresponds to a decrease in the size of the observed inhomogeneities. The dependence of the broadening Δf_D on the scattering wave number q at fixed disk rotation speeds (points 1 and 2 for $n_2 = 25$ and 15) is shown in Fig. 6, from which it is evident that this dependence corresponds approximately to the relation $\omega(q) \sim q^{2/3}$ (lines); this implies that smaller inhomogeneities, which correspond to large scattering wave numbers, are shorter-lived, and an increase in the rotation speed shortens the lifetime of inhomogeneities having a fixed characteristic scale.

It should also be noted that the exact relation $\Delta f_D = \omega(q)$ can be used to determine the average rate of dissipation of kinetic energy according to the equation $\epsilon = (\Delta f_D/0.42q^{2/3})^3$. Consequently, the measurement of the spectral characteristics of radiation scattered in a

fluid flow yields information about certain aspects of the temporal and spatial nature of the density fluctuations generated in the evolution of turbulent flow.

LITERATURE CITED

1. Yu. N. Dubnishchev and B. S. Rinkevichus, *Methods of Laser Doppler Anemometry* [in Russian], Nauka, Moscow (1982).
2. V. V. Protopopov and N. D. Ustinov, *Laser Heterodyning* [in Russian], Nauka, Moscow (1985).
3. H. L. Frisch, "Study of turbulence by spectral fine structure of scattered light," *Phys. Rev. Lett.*, 19, No. 22 (1967).
4. Dzh. Benedek, "Optical mixing spectroscopy and its applications to problems of physics, chemistry, biology, and engineering," *Usp. Fiz. Nauk*, 106, No. 3 (1972).
5. B. Crosignani, P. Di Porto, and M. Bertolotti, *Statistical Properties of Scattered Light*, Academic Press, New York (1975).
6. V. P. Solov'ev, "Spectrum of light scattered by a turbulent fluid," in: *Molecular Physics of Nonequilibrium Systems* [in Russian], IT Sib. Otd. Akad. Nauk SSSR, Novosibirsk (1984).
7. A. Yoshizawa, "A statistical investigation of shear turbulence: the Reynolds-stress transport equation," *J. Phys. Soc. Jpn.*, 51, No. 2 (1982).
8. V. P. Klochkov, L. F. Kozlov, I. V. Potykevich, and M. S. Soskin, *Laser Anemometry, Remote Spectroscopy and Interferometry* [in Russian], Naukova Dumka, Kiev (1985).
9. A. M. D'yakonov, Yu. S. Kapshin, V. V. Klyubin, et al., "Laser heterodyne spectrometers for the analysis of scattered light," *LIYaF, Akad. Nauk SSSR Preprint No. 427* [in Russian], B. P. Konstantinov Institute of Nuclear Physics, Academy of Sciences of the USSR, Leningrad (1978).
10. H. Schlichting, *Boundary-Layer Theory*, 6th ed., McGraw-Hill, New York (1968).
11. B. I. Fedorov, G. Z. Plavnik, I. V. Prokhorov, and L. G. Zhukhovitskii, "Transition flow regime on a rotating disk," *Inzh.-fiz. Zh.*, 31, No. 6 (1976).
12. R. Kobayashi, Y. Kohama, and Ch. Takamada, "Spiral vortices in boundary layer transition regime on rotating disk," *Acta Mech.*, 35, No. 1 (1980).

FLOW DIAGNOSTICS IN A CRYOGENIC WIND TUNNEL

S. Yu. Borisov, A. L. Iskra, V. P. Kulesh,
and A. M. Naumov

UDC 533.6.071.6

In the construction and setting up of a cryogenic wind tunnel an important consideration is to ensure good flow quality. This paper presents results of an experimental investigation to study the causes and conditions for the occurrence of two-phase flow in the T-04 cryogenic wind tunnel [1, 2], and to determine the operating flow regime of this facility to give the purest flow.

A schematic diagram of the T-04 facility is given in Fig. 1: 1) working section of dimensions 200 × 200 × 740 mm, 2) pressure chamber; 3) ejector; 4) return channel; 5) sprayer for atomizing liquid nitrogen; 6) compressed air tank; 7) diffuser; 8) noise-suppressing ventilation shaft; 9) liquid air tank; 10) regenerator bank.

Initial cooling of the tunnel body, the pipes, and regenerator fittings was performed by injecting liquid nitrogen into the stream. The cold regeneration system ensured cooling of the ejected air, and heating of the gas exhausted from the tunnel. Sequential switching of the three regenerators ensured that the flow cryogenic temperature is maintained for a long time with the sprayers switched off. The tunnel can be operated even without the cold regeneration system. In that case the air goes to the ejector, bypassing the regenerator bank, and gas is removed from the tunnel simultaneously through all the regenerators.

Zukovskii. Translated from *Zhurnal Prikladnoi Mekhaniki i Tekhnicheskoi Fiziki*, No. 3, pp. 169-172, May-June, 1991. Original article submitted January 11, 1989; revision submitted November 10, 1989.